Time Course of Skeletal Muscle Glucose Uptake During Euglycemic Hyperinsulinemia in the Anesthetized Rabbit: A Fluorine-18-2-Deoxy-2-Fluoro-D-Glucose Study

Kurt A. Mossberg and Heinrich Taegtmeyer

Division of Cardiology, Department of Medicine, University of Texas Health Science Center, Houston, Texas

Since skeletal muscle has been implicated as the major site of insulin resistance, the purpose of this study was to examine in detail the time course of muscle glucose uptake during the onset and maintenance of euglycemic hyperinsulinemia. Uptake of ^{18}F-2-deoxy-2-fluoro-D-glucose (FDG) by the thigh muscle of an anesthetized rabbit was monitored by a single pair of coincidence photon detectors. Graphical analysis of tissue and plasma radioactivity concentrations was performed to derive fractional rates of FDG phosphorylation continuously. FDG phosphorylation rates were determined during rest (glucose 7 m*M*, insulin 5–10 μU/ml) and subsequent 5-min intervals under conditions of euglycemic hyperinsulinemia (glucose 6–8 m*M*; insulin 350–400 μU/ml plasma). FDG phosphorylation did not increase above resting control levels until 5.5 ± 1.5 min after intravenous insulin administration. After 20–30 min of hyperinsulinemia, FDG phosphorylation and calculated glucose metabolic rates were increased by 50%. At 35–40 min of the clamp in place, there was a second increase in tracer phosphorylation which plateaued at 200% of control ($p < 0.01$) and remained at this level for the remainder of the experiment. In conclusion, we have described a method for making rapid, serial estimates of insulin-mediated skeletal muscle glucose uptake. We suggest that appraisal of the time course of glucose uptake with FDG will aid in the understanding of normal and pathophysiologic states of insulin action in vivo.

J Nucl Med 1992; 33:1523–1529

The euglycemic hyperinsulinemic clamp technique is a well-accepted method for the assessment of whole-body insulin-mediated glucose metabolism. However, the technique by itself does not allow for the differential monitoring of glucose utilization by individual tissues. Tissues other than the liver have been shown to be the major sites of insulin-stimulated glucose disposal (*1–3*), making it important to isolate the various peripheral components in order to study their contribution to overall glucose homeostasis. Recently, Shulman and colleagues demonstrated with nuclear magnetic resonance (NMR) spectroscopy that the defect in glucose disposal in patients with noninsulin-dependent diabetes mellitus (NIDDM) is reflected in decreased skeletal muscle glycogen synthesis (*4*), which emphasized the importance of muscle in whole body glucose uptake. Conventional methods for selectively studying skeletal muscle glucose uptake in vivo require arterial and venous catheterizations, in addition to needle biopsies, which makes routine clinical application impractical.

We recently reported on the use of positron emitting fluorodeoxyglucose (FDG) for the noninvasive study of muscle glucose uptake under steady-state resting conditions (*5*). Since skeletal muscle is the predominant tissue in the limbs, one has a relatively homogeneous region of interest that eliminates the need for spatial resolution. Our previous study demonstrated that the rate of tissue accumulation (trapping) of FDG could be monitored on a second-by-second basis. However, our ability to quantitate rates of FDG phosphorylation, and thereby estimate glucose disposal, was limited to data acquisitions under steady-state resting conditions of relatively long duration. We have since developed a system that provides better temporal resolution, enabling accurate quantitation of tracer uptake during shorter time intervals. The new system permits more detailed temporal study during an acute metabolic perturbation and should therefore assist in the development of new theoretical models (*6*) of insulin action. The purpose of this investigation was to monitor skeletal muscle FDG uptake in a rapid serial manner during resting control conditions followed by the onset and maintenance of a euglycemic hyperinsulinemic clamp in an anesthetized rabbit. In addition, we also examined the reproducibility of this method under resting conditions.

Received Nov. 8, 1991; revision accepted Mar. 25, 1992.

For reprints contact: Kurt A. Mossberg, PhD, Department of Physical Therapy, School of Allied Health Sciences J-28, University of Texas Medical Branch, Galveston, TX 77550-2782.

METHODS

Animal Preparation

Male New Zealand white rabbits (Ray Nichols Rabbitry, Lumberton, TX) weighing 3–4 kg were studied after a 16–20-hr fast. Details of the animal preparation have been published previously (*5*). Twenty minutes prior to the administration of general anesthesia, the animals received an intramuscular injection of dihydroergotamine to prevent the stress-induced hyperglycemia that accompanies anesthesia and surgical catheterization. We have previously reported that this intervention results in a pharmacologic euglycemic clamp with minimal to no interference in other metabolic or hemodynamic parameters (*7*). Heart rate and mean arterial pressure were monitored continuously to ascertain the hemodynamic stability of the preparation.

Production and Measurement of Radioactivity

Fluorine-18 was produced by the ^{18}O (p,n) ^{18}F reaction at the University of Texas Health Science Center cyclotron. Fluorine-18-labeled FDG was then synthesized by the method of Hamacher et al (*8*). The specific activity of FDG was >5,000 Ci/mmol and radiochemical purity was 99% as determined by HPLC. FDG was administered as a 3 ml bolus (150–300 μCi) given over 30 sec followed by a continuous infusion of tracer for the duration of the data acquisition. Continuous infusion of tracer was necessary to insure an adequate concentration of tracer in the plasma during the clamp.

Tissue radioactivity in the form of coincidence gamma photons was measured as previously described (*9*). Counts per second were converted to μCi/ml of tissue volume using a calibration bar phantom that approximated the size and volume of the hindlimb. Arterial radioactivity concentrations were determined by direct measurement of ^{18}F positrons (*9*) as blood was shunted between the right femoral artery and vein across a shielded scintillation disc. The plasma radioactivity concentration was derived later by correcting for the hematocrit and the rate of red blood cell uptake of FDG. After appropriate calibration, counts/sec were converted to μCi/ml plasma.

Graphical Analysis

The graphical analysis technique of Patlak and colleagues (*10*, *11*) was employed to quantitate the fractional rate of tracer phosphorylation. Briefly, the slope of the relationship between the integral of the plasma radioactivity concentration (μCi/ml plasma/min) and the tissue radioactivity concentration (μCi/ml tissue) during any given time interval yields the transfer constant, K, or the fractional rate of FDG phosphorylation (ml plasma/min/ml tissue) (*5*). Multiplication of K by the plasma glucose concentration gives an index of the rate of glucose uptake (Rg) in μmol/min/ml tissue. K itself is also considered an index of glucose clearance (*7*). Because of inherent differences in the kinetics of transport and phosphorylation of glucose and the FDG analog, we emphasize that measures of glucose uptake and clearance are referred to as indices (see discussion below). Slope derivations during successive 5-min intervals were possible due to high temporal resolution (seconds) of both tissue and plasma radioactivity concentrations.

After administration of FDG, 10–15 min were necessary for complete equilibration of tracer between plasma and tissue spaces. Following equilibration, the resting fractional rate of FDG phosphorylation was derived in a 5–8-min interval immediately prior to insulin administration. The model assumes steady-state conditions during the time interval in which the slope calculation is made. The rapid sampling of both tissue and plasma radioactivity concentrations provided a data point at least every 30 sec during graphical analysis. Thus, we were able to minimize the time interval over which slope derivations were made. This was especially important since steady state became relatively transient after insulin stimulation. Goodness of fit was assessed by analyzing the residual sum of squares.

Euglycemic Hyperinsulinemic Clamp

The clamp was initiated 20 min after the administration of FDG. This allowed enough time for tracer equilibration and the derivation of a reliable rate of FDG phosphorylation under resting, basal conditions. We followed the clamp protocol of DeFronzo and colleagues (*12*) with slight modifications. Briefly, hyperinsulinemia was brought about by bolus injection of 200 μU insulin per kg body weight into the external jugular vein followed immediately by an insulin infusion of 20 μU/kg/min. Four minutes after insulin administration, an infusion of glucose (200 mg/ml) was begun with an initial pump setting of 0.05 ml/min and thereafter adjusted every five minutes accordingly (*12*).

Analytical Procedures

Arterial blood was sampled from the carotid artery for determination of plasma glucose every 5 min after the administration of insulin. Blood was immediately centrifuged and the supernatant fraction analyzed for glucose using an automated microanalyzer (Model 2300GL, YSI, Yellow Springs, OH). Arterial blood was also sampled every 20 min for determination of nonesterified fatty acids (NEFA) and insulin. These samples were frozen at −70°C for later analyses (NEFA, NEFA-C, Wako Pure Chemical, Osaka, Japan; insulin, Phedaseph, Pharmacia Diagnostics, Piscataway, NJ).

Data Analysis

Fractional rates of FDG phosphorylation were determined for successive 5-min intervals in both control (n = 5) and insulin-stimulated animals (n = 4) and are presented as a percentage of the resting value. The reproducibility of the method was estimated by calculating the pooled variance for the repeated measures (*13*) of FDG phosphorylation in the control group according to the following equation (*14*):

$$s^2_p = \sum s^2(n-1)/\sum (n-1), \qquad \text{Eq. 1}$$

where s^2_p is the pooled variance. The CV was calculated as:

$$CV = (\sqrt{s^2_p}/X_p) \times 100, \qquad \text{Eq. 2}$$

where X_p is the pooled mean rate of FDG phosphorylation.

A split-plot, two-way analysis of variance (repeated measures across time) was employed to determine the existence of significant differences across time intervals and between the two groups as well as a significant interaction between time and treatment (*15*) for both FDG phosphorylation and glucose utilization. A significant F ratio for time was followed by Newman-Keul's procedure to allow for all pair-wise comparisons at each time interval. Statistical analyses were performed using a personal computer software program (Statpak 4.1, Northwest Analytical; Portland, OR). All results are reported as means ± s.e.

RESULTS

Figure 1 shows (from top to bottom) the circulating plasma-insulin, plasma-glucose concentrations and the

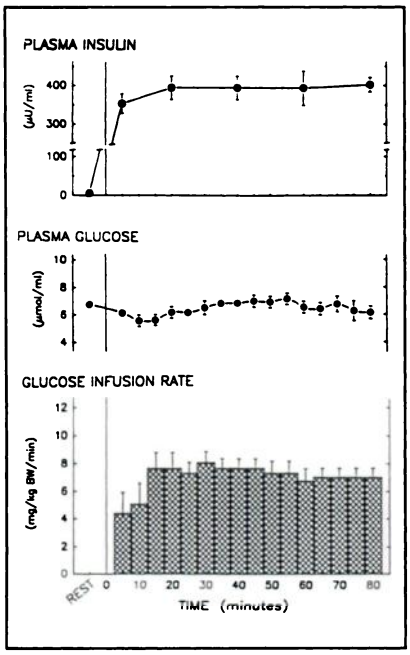

FIGURE 1. Circulating plasma insulin and glucose and the glucose infusion rate during euglycemic hyperinsulinemia (n = 4). Values are mean ± s.e.

glucose infusion rate for insulin-treated animals. Plasma-insulin in control animals ranged from 5 to 10 μU/ml for the duration of each experiment, while under clamp conditions insulin was increased to levels that ranged from 350 to 400 μU/ml. Glucose levels were steady for the duration of the experiment and averaged 7 m*M*. In order to maintain euglycemia, glucose infusion rates were increased rapidly and then leveled off within 15–20 min and remained constant at 7–8 mg/kg BW/min. NEFA ranged from 0.5 to 1.0 μeq/ml (data not shown) and tended to be lower in insulin treated animals as compared to controls. The differences in NEFA were not statistically significant. Therefore, we assume they did not account for differences in FDG phosphorylation or glucose uptake.

A summary of the fractional rates of FDG phosphorylation for all experiments is illustrated in Figure 2. Shown as a percent of the resting interval, insulin-treated animals demonstrated no increase in tracer uptake in the first 5 min. Beginning in the 5–10-min interval of the clamp, an observable (but statistically nonsignificant) increase in FDG uptake occurred and continued for another 5–10 min until it plateaued at 150% of rest. A second, further increase in FDG phosphorylation occurred beginning 35–40 min after insulin administration and plateaued at approximately 200% above resting. This second increase resulted in significant elevations in the rate of tracer uptake ($p < 0.01$). Factorial analysis revealed a significant interaction ($p < 0.01$), indicating that the insulin response was influenced by the time of exposure.

Figure 3 illustrates the results of the graphical analysis between 1 and 30 min after FDG injection for an individual control experiment (panel A) and an individual clamp experiment (panel B). Equilibration was complete within 10 min after tracer administration in these two experiments. In all experiments, equilibration was complete within 15 min. Differences in the time and characteristics of the equilibration phase resulted from differences in FDG bolus distribution between animals. In the two experiments shown in Figure 3, resting or basal uptake was equal to the slope of the 12–20-min interval after the injection of FDG. Direct comparisons of absolute slopes cannot be made between animals as will be discussed further. Measurement of the resting rate of FDG phosphorylation from this time interval proved to be reliable, because no further changes in slope occurred after this time interval in control experiments (Fig. 3A).

Determination of the time of onset of the insulin response was made by examining each curve, point-by-point, after the initiation of the clamp. The time at which a consistent, protracted increase in slope occurred with re-

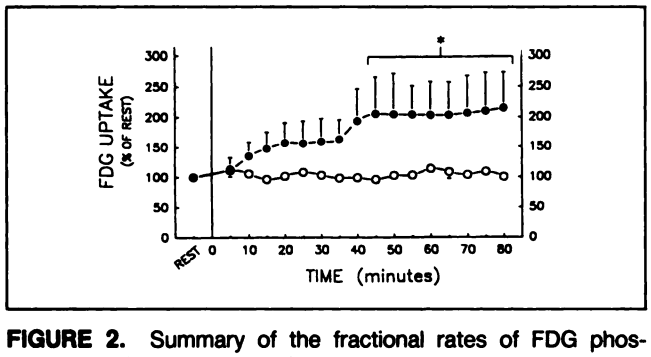

FIGURE 2. Summary of the fractional rates of FDG phosphorylation for control (n = 5, open symbols) and insulin-treated (n = 4, closed symbols) animals. Time zero is the onset of hyperinsulinemia. Values are mean ± s.e. (* $p < 0.01$).

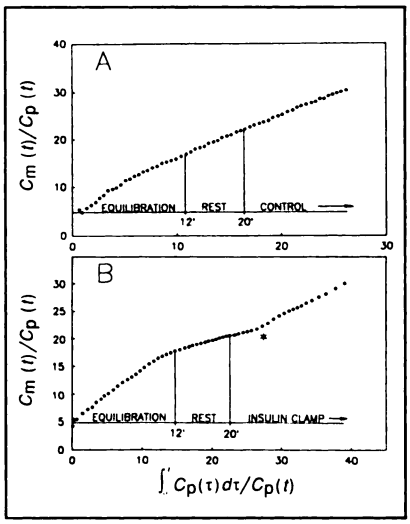

FIGURE 3. Representative plots of the fractional rate of FDG phosphorylation in a control animal (A) and an insulin treated animal (B). Points are plotted every 30 sec beginning at 1 min and ending at 30 min after FDG administration. (Note: the abscissa does not equate with time.) The resting slope calculation was made during the 12–20-min interval following injection and equilibration of FDG. Hyperinsulinemia commenced at 20 min and the asterisk denotes the time at which the protracted increase in FDG phosphorylation occurred (4.5 min after insulin injection for this experiment).

spect to the resting interval was defined as the insulin response delay time (asterisk, Fig. 3B). Table 1 lists the delay times for the initial response (mean = 5.5 ± 1.5 min) as well as the late response (approximately 35–40 min) in the four clamp experiments.

Mean rates of the glucose uptake index (Rg) for control and clamp experiments are shown in Figure 4. With hyperinsulinemia, there was no increase in Rg index in the first 10 min of insulin exposure. This was followed by increases similar to those seen for FDG phosphorylation in the remainder of the data acquisition. Because of the variability in both plasma-glucose and FDG phosphorylation and the fact that these variabilities were compounded when calculating Rg, the differences were not statistically significant.

The discrepancy between the time course of FDG phosphorylation and Rg index in the first 10 min of hyperinsulinemia could be due to two factors. First, at the time of the initial increase in the rate of FDG phosphorylation, there was a slight decrease in plasma glucose. Thus, the discrepancy could be explained simply on mathematical grounds (since the Rg index is the product of the fractional rate of FDG phosphorylation and plasma-glucose concentration) and illustrates the importance of the mass action effect of the plasma-glucose concentration (*16*). A second factor responsible for the discrepancy could be a change in the ratio of FDG to glucose in the plasma. FDG was infused continuously from the outset of the data acquisition, whereas glucose infusion was not begun until 4 min after injection of insulin. An increase in the ratio of tracer to tracee would enhance the ability of FDG to compete with glucose for transport and phosphorylation sites. However, as Figure 5 illustrates, this was not the case because FDG levels began to fall within 2–3 min after insulin injection, and the most rapid fall occurred at 6–7 min despite increasing rates of tracer infusion that paralleled the rate of glucose infusion.

We also assessed the reproducibility of measuring the fractional rate of FDG phosphorylation (glucose clearance index) and the Rg index in the five control experiments according to Equations 1 and 2. The overall means and variances for the individual experiments are shown in Table 2. The reproducibility in terms of the coefficient of variation derived from the pooled variance and mean for the 16 repeated measures of FDG phosphorylation was 10.8%. The reproducibility of the Rg index across the time points for which plasma-glucose concentrations were determined in the control experiments was 5.7%.

TABLE 1
Response Times in Minutes to Acute Insulin Stimulation

Exp	Initial	Late
1	7.0	40–45
2	6.5	30–35
3	4.5	35–40
4	3.5	35–40

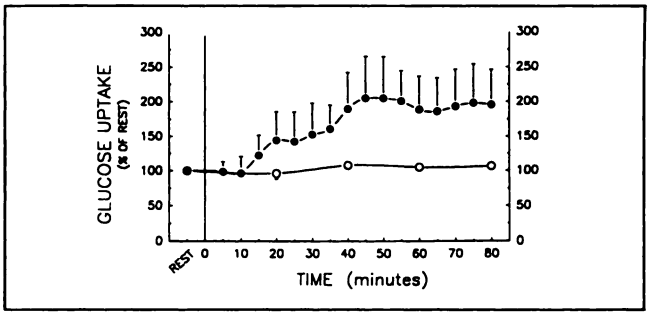

FIGURE 4. Glucose uptake index (Rg) for control (n = 5, open symbols) and clamp experiments (n = 4, closed symbols). Time zero is the onset of hyperinsulinemia. Values are mean ± s.e.

DISCUSSION

We have described a novel application of positron-emitting ^{18}F-labeled 2-deoxyglucose for the noninvasive study of glucose uptake in response to an acute insulin stimulus. We believe this is the first quantitative estimation of the time course of glucose uptake by muscle in vivo on a minute-to-minute basis. Serial monitoring of FDG radioactivity with externally placed radiation detectors allowed for direct comparison of estimates of glucose uptake under control and euglycemic hyperinsulinemic conditions. The time course of tracer uptake suggests that: (1) the initial insulin response is delayed approximately 5–6 min and (2) there is a second increase that occurs approximately 35–40 min after insulin stimulation resulting in a two-fold increase in the rate of glucose utilization.

As previously stated, the methods provide indices rather than absolute rates of glucose clearance and uptake. Two factors are responsible for this limitation. The first relates to differences in the uptake kinetics of glucose and the FDG analog. The relationship of the steady-state rate of phosphorylation of the analog to the net utilization rate of glucose has been termed the lumped constant (LC) (*17*). While there are no reports of LC determinations for FDG in skeletal muscle, tritium-labeled 2-deoxyglucose has been shown to have a LC ranging from 0.76 to 1.05 under resting conditions (*18,19*). More importantly, the LC was not found to change significantly with physiologic (*20*) or

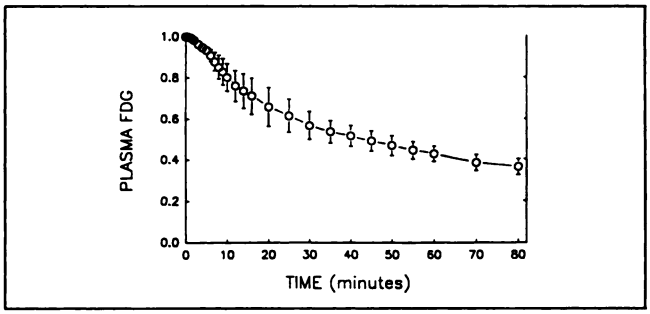

FIGURE 5. Plasma FDG levels as a fraction of radioactivity concentration present at the onset of hyperinsulinemia. Values are mean ± s.e.

TABLE 2
Overall Means and Variances for Repeated Measures of FDG Phosphorylation and Glucose Uptake Index (Rg) During Control Intervals (Pooled means and variances are included)

	FDG Phosphorylation		Rg Index	
Exp	Mean	s^2	Mean	s^2
1	111	129.3	114	37.7
2	108	98.7	105	6.2
3	97	243.9	97	262.2
4	101	48.9	100	15.0
5	99	102.0	104	107.0
X_p	103		104	
s^2_p		124.6		35.7

pharmacologic (*19*) levels of insulin. Unfortunately, due to technical difficulties nearly all LC determinations for skeletal muscle, as well as other organs, have been performed using in-vitro preparations, with glucose as the sole energy-providing substrate.

In spite of the in-vitro data, changes in the LC are possible due to hyperinsulinemia in vivo. Furthermore, it becomes important to know when the change in the LC might occur. As the rate limiting step in glucose metabolism is shifted from transport to some further step in metabolism, the control strengths of transport and phosphorylation might shift. These shifts would be expected to occur at the same time as the insulin-induced increase in hexose transport. Therefore, one would expect a similar time course for glucose uptake as observed for FDG, but with a possible difference in the magnitude of uptake as the LC changed. In-vivo validation will require assessment of free and phosphorylated hexose in freeze clamped tissue, as well as analysis of the kinetics of insulin-sensitive and insensitive transporter species, at specific time points after insulin administration.

The second factor that necessitates reporting indices rather than absolute values relates to the conversion of tissue coincidence cps to μCi/ml. Accurate conversion of count rates to tissue radioactivity concentration requires the calibration bar phantom be the exact dimensions of the hindlimb. Since the geometry of each hindlimb is unique, the phantom can only approximate the volume and dimensions of the limb. In addition, the slightest differences in placement of hindlimbs within the detector field of view can affect the conversion. To overcome these inevitable geometric deviations, each animal served as its own control, such that, prior to any intervention, a "resting" rate of tracer uptake was derived. All subsequent rates were compared to and reported as a percentage of the resting interval. We believe that direct comparison with a resting control interval determined for the same animal has obvious advantages that far outweigh this limitation.

Reliable measures of the resting rate of FDG uptake would be reflected by little or no change in rates of uptake later in time in control experiments (Fig. 2). Other reliability reports using the coefficient of variation of the pooled variance for repeat measurements found that measures of glycogen content via needle biopsy (*14*) had a percent deviation of 8.6%, while a NMR spectroscopy method (*21*) had a deviation of 6.5%. Because glycogen content is a concentration, one would expect that it changed very little over the time intervals used for calculations in these studies. In contrast, hexose uptake is a rate that likely oscillates at varying frequencies in intact systems. Therefore, we believe the method demonstrates a sufficient level of reproducibility. Furthermore, the discrepancy between the reliability of clearance vs uptake measures was simply the result of chance and the apparent oscillation. In controls, the Rg index was determined at a limited number of time points coinciding with plasma-glucose measures (every 20 min). Assessing the reliability in terms of clearance for those same time points resulted in a percent deviation of 3.6% (4 time points) as opposed to 10.8% (16 time points).

The insulin effect in vivo requires that a number of specific events take place beginning with insulin transport across the capillary endothelium (*22*), receptor binding (*23*), tyrosine kinase activation (*24*) and further intracellular signalling leading to recruitment (*25*) and activation of glucose transport proteins and ultimately phosphorylation by hexokinase (the committed step in glucose disposal). The first step in this cascade is the movement of insulin from blood to the cell membrane. Recently, Bergman and colleagues (*26*), using a canine model, provided evidence indicating that transport of insulin across the capillary endothelium may account for the approximate 10–12 min delay in whole-body glucose disposal after insulin administration. Our observation of a 5–6-min delay is consistent with the changes observed in lymph insulin (*26*), given the different events being measured and their sites of measurement. We believe the observed delay in FDG phosphorylation is, at least in part, due to the transport of insulin from blood to muscle cell receptor.

Other factors that must be considered as potentially contributing to the delay time are related to the initiation of intracellular events. Studies in isolated adipocytes have shown that approximately 5–6 min are necessary before maximal recruitment of cytochalasin B binding sites to

the plasma membrane in response to insulin (*27*). In these same studies, the increase in cytochalasin B binding sites in the plasma membrane preceded the increase in 3-O-methylglucose transport by approximately 2–3 min. The time to maximum transport took slightly less than 10 min and is consistent with our finding of a 10–15-min period of time elapsing before the initial plateau in glucose clearance was attained. The slight difference in timing could be attributed to the in-vitro preparation presumably having a more sudden acceleration of events with the addition of pharmacologic levels of insulin to the incubation medium.

An unexpected finding was the second, later increase in the rate of FDG uptake that occurred after the initial plateau. Evidence from other investigations supporting an insulin-induced step-wise increase in glucose utilization comes from time course studies of protein kinase C (PKC), a putative component of the intracellular signalling process. Cooper and associates (*28*) demonstrated in myocytes a cyclical response of membrane bound PKC in addition to an initial rise, plateau and second increase in cytosolic PKC. The initial change took place over 1–2 min and the subsequent changes occurred after 10 min. Saltiel and coworkers (*29*) observed similar cyclical changes occurring in myocyte production of diacylglycerol in response to insulin stimulation. While these reported changes were demonstrated in vitro and occurred over shorter time intervals, the time differences could be reconciled by the fact that these measured responses are presumably steps that occur some time before an observable acceleration in glucose disposal.

The later increase also could have been due to a change in the ratio of FDG to glucose, but the glucose concentration was not changing at this time and the plasma FDG was falling. Also, sudden changes in NEFA would necessitate a greater reliance on glucose for energy needs, but these were not observed. Although the possibility exists that changes in NEFA were missed due to infrequent sampling, plasma levels at 20, 40 and 60 min were unchanged.

The overall response to hyperinsulinemia could have been due to other neurohumoral changes not directly measured in this study. An increase in glucagon could have occurred in response to the initial slight fall in plasma glucose. Others have shown, however, that elevated plasma glucagon has no effect on skeletal muscle glucose uptake (*30,31*). In addition, glucagon tends to raise fatty acid levels and we did not observe any change in NEFA. Moreover, heart rate and mean arterial pressure did not change in such a way as to indicate an insulin effect on catecholamines.

The possibility exists that changes in the rate of FDG uptake could have been due to changes in tissue radioactivity in the exchangeable compartments, i.e., vascular and interstitial fluid spaces. We have unpublished data from labeled sucrose experiments indicating that hyperinsulinemia does not change the size of the extracellular fluid space in muscle. Previously, we reported that hyperinsulinemia increases skeletal muscle blood flow approximately two-fold (*32*). We have also made preliminary observations on the time course of muscle blood flow and glucose uptake with the onset of contractile activity and found immediate increases in flow (5–10-fold) but delays in glucose uptake similar to those reported here. These data indicate that the method of analysis is insensitive to changes in vascular and interstitial volumes (*10*).

Previous reports of whole-body glucose uptake kinetics have suggested that insulin action is delayed by several minutes (*33,34*). The notion of a delay has, however, been based on changes in glucose infusion rates and the time to reach steady state uptake under clamp conditions. More specifically, the time course of leg glucose uptake has been found to be significantly delayed in diabetic subjects, but the frequency of measurements was limited to 20 min intervals (*1*). It would be of interest to examine the time course of FDG uptake in the diabetic state to assess the relationship between disease severity and delay time.

Due to the lack of temporal resolution, there has thus far been no direct evidence related to muscle-specific time courses of glucose uptake detailing the exact onset of the insulin response. By using the FDG tracer analog, we have demonstrated that the time course of skeletal muscle glucose uptake in response to acute hyperinsulinemia can be estimated and as a result may provide new information on the skeletal muscle insulin response.

ACKNOWLEDGMENTS

This work was supported in part by a grant-in-aid from the American Heart Association—Texas Affiliate and USPHS grant R01-HL43133. We thank Dr. Timothy Tewson and his cyclotron staff for the preparation of FDG and Jane Mommessin for expert technical assistance.

REFERENCES

1. DeFronzo R, Gunnarsson R, Bjorkman O, Olsson M, Wahren J. Effects of insulin on peripheral and splanchnic glucose metabolism in noninsulin dependent (type II) diabetes mellitus. *J Clin Invest* 1985;76:149–155.
2. DeFronzo R, Jalot E, Jequier E, Maeder E, Wahren J, Felig P. The effect of insulin on the disposal of intravenous glucose. *Diabetes* 1981;30: 1000–1007.
3. Katz L, Glickman M, Rapoport S, Ferrannini E, DeFronzo R. Splanchnic and peripheral disposal of oral glucose in man. *Diabetes* 1983;32: 675–679.
4. Shulman G, Rothman D, Jue T, Stein P, DeFronzo R, Shulman R. Quantitation of muscle glycogen synthesis in normal subjects and subjects with non-insulin-dependent diabetes by ^{13}C nuclear magnetic resonance spectroscopy. *N Engl J Med* 1990;322:223–228.
5. Mossberg KA, Rowe RW, Tewson TJ, Taegtmeyer H. Rabbit hindlimb glucose uptake assessed with positron emitting fluorodeoxyglucose. *J Appl Physiol* 1989;67:1569–1577.
6. Bass L. Heterogeneity within observed regions: physiologic basis and effects on estimation of rates of biodynamic processes. *Circulation* 1985; 72(suppl IV):IV-47–IV-52.
7. Mossberg KA, Taegtmeyer H. Dihydroergotamine as a pharmacologic euglycemic clamp in the surgically traumatized rabbit. *Metabolism* 1991; 40:594–599.
8. Hamacher K, Coenen H, Stocklin G. Efficient stereospecific synthesis of no-carrier added 2-[^{18}F]-fluoro-2-deoxy-D-glucose using aminopolyether

supported nucleophilic substitution. *J Nucl Med* 1986;27:235–238.
9. Nguyen V, Mossberg K, Tewson T, et al. Temporal analysis of myocardial glucose metabolism by ^{18}F-2-deoxy-2-fluoro-D-glucose. *Am J Physiol* 1990; H1022–H1031.
10. Patlak CS, Blasberg RG, Fenstermacher JD. Graphical evaluation of blood-to-brain transfer constants from multiple-time uptake data. *J Cereb Blood Flow Metab* 1983;3:1–7.
11. Patlak CS, Blasberg RG. Graphical evaluation of blood-to-brain transfer constants from multiple-time uptake data. Generalizations. *J Cereb Blood Flow Metab* 1985;5:584–590.
12. DeFronzo R, Tobin J, Andres R. Glucose clamp technique: a method for quantifying insulin secretion and resistance. *Am J Physiol* 1979;237: E214–E223.
13. Snedecor G, Cochran W. *Statistical methods*, 6th edition. Ames, IA: The Iowa State University Press; 1967:593.
14. Harris R, Hultman E, Nordesjo L-O. Glycogen, glycolytic intermediates and high energy phosphates determined in biopsy samples of musculus quadriceps of man at rest. Methods and variance of values. *Scand J Clin Lab Invest* 1974;33:109–120.
15. Zar J. *Biostatistical analysis*, 2nd edition. Inglewood Cliffs: Prentice-Hall, Inc.; 1984:163–168.
16. Soskin S, Levine R. A relationship between the blood sugar level and the fate of sugar utilization, affecting the theories of diabetes. *Am J Physiol* 1937;120:761–770.
17. Sokoloff L, Reivich M, Kennedy C, et al. The [^{14}C]deoxyglucose method for the measurement of local cerebral glucose utilization: theory, procedure, and normal values in the conscious and anesthetized albino rat. *J Neurochem* 1977;28:897–916.
18. Burnol A-F, Ferre P, Leturque A, Girard J. Effect of insulin on in vivo glucose utilization in individual tissues of anesthetized lactating rats. *Am J Physiol* 1987;252:E183–E188.
19. Ferre P, Leturque A, Burnol A-F, Penicaud L, Girard J. A method to quantify glucose utilization in vivo in skeletal muscle and white adipose tissue of the anesthetized rat. *Biochem J* 1985;228:103–110.
20. Meszaros K, Bagby G, Lang C, Spitzer J. Increased uptake and phosphorylation of 2-deoxyglucose by skeletal muscles in endotoxin treated rats. *Am J Physiol* 1987;253:E33–E39.
21. Price T, Rothman D, Avison M, Buonamico P, Shulman R. ^{13}C-NMR measurements of muscle glycogen during low-intensity exercise. *J Appl Physiol* 1991;70:1836–1844.
22. King G, Johnson S. Receptor-mediated transport of insulin across endothelial cells. *Science* 1985;227:1583–1586.
23. Prager R, Wallace P, Olefsky J. In vivo kinetics of insulin action on peripheral glucose disposal and hepatic glucose output in normal and obese subjects. *J Clin Invest* 1986;78:472–481.
24. Kasuga M, Fujita-Yamaguchi Y, Blithe D, Kahn C. Tyrosine-specific protein kinase activity is associated with the purified insulin receptor. *Proc Natl Acad Sci USA* 1983;80:2137–2141.
25. Wardzala L, Jeanrenaud B. Potential mechanism of insulin action on glucose transport in the isolated rat diaphragm: apparent translocation of intracellular transport units to the plasma membrane. *J. Biol Chem* 1981; 256:7090–7093.
26. Yang Y, Hope I, Ader M, Bergman R. Insulin transport across capillaries is rate limiting for insulin action in dogs. *J Clin Invest* 1989;84: 1620–1628.
27. Karnieli E, Zarnowski M, Hissin P, Simpson I, Salans L, Cushman S. Insulin-stimulated translocation of glucose transport systems in the isolated rat adipose cell. *J Biol Chem* 1981;256:4772–4777.
28. Cooper D, Konda T, Standaert M, Davis J, Pollett R, Farese R. Insulin increases membrane and cytosolic protein kinase C activity in BC3H-1 myocytes. *J Biol Chem* 1987;262:3633–3639.
29. Saltiel A, Sherlin P, Fox J. Insulin-stimulated diacylglycerol production results from the hydrolysis of a novel phosphatidylinositol glycan. *J Biol Chem* 1987;262:1116–1121.
30. Pozefsky T, Tancredi RG, Moxley RT, et al. Metabolism of forearm tissues in man. Studies with glucagon. *Diabetes* 1976;25:128–135.
31. Daniel PM, Pratt DE, Spargo E. The mechanism by which glucagon induces release of amino acids from muscle and its relevance to fasting. *Proc R Soc Lond* 1977;196:347–365.
32. Mossberg KA, Mullani N, Gould KL, Taegtmeyer H. Skeletal muscle blood flow in vivo: detection with rubidium-82 and effects of glucose, insulin and exercise. *J Nucl Med* 1987;28:1155–1163.
33. Doberne L, Greenfield M, Schulz B, Reaven G. Enhanced glucose utilization during prolonged clamp studies. *Diabetes* 1981;30:829–835.
34. Sherwin R, Kramer K, Tobin J, et al. A model of kinetics of insulin in man. *J Clin Invest* 1974;53:1481–1492.